

Vacuum Ultraviolet Dual-Comb Spectroscopy

John J. McCauley^{1†}, Dylan P. Tooley^{1,2†}, R. Jason Jones^{1*}

¹James C. Wyant College of Optical Sciences, University of Arizona, Tucson, AZ 85721, USA.

²Department of Physics, University of Arizona, Tucson, AZ 85721, USA.

*Corresponding author(s). E-mail(s): rjjones@arizona.edu;

†These authors contributed equally to this work.

Abstract

The optical frequency comb has made a significant impact in precision spectroscopy and on our ability to probe atomic, molecular and, recently, nuclear transitions to further our understanding of their fundamental properties and how their dynamics and complex interactions affect the observed world. To expand the energy scales and types of systems that can be studied, frequency comb sources from terahertz to vacuum ultraviolet frequencies and beyond have been pursued. Dual-comb spectroscopy, enabled by the development of these frequency comb sources, allows broadband absorption measurements of complicated spectra, exceeding the limitations of direct, single-comb spectroscopy. To date, however, the dual-comb approach has not been able to directly access many important transitions that lie at challenging vacuum ultraviolet wavelengths. Here, we demonstrate dual-comb spectroscopy in the vacuum ultraviolet utilizing intracavity high harmonic generation. This multi-harmonic source is used to measure molecular absorbance spectra at $\lambda = 210$ nm and $\lambda = 149$ nm from room-temperature samples of acetylene and ammonia, respectively. These measurements resolve the Doppler broadened structure of congested molecular spectra with absolute frequency accuracy. Noise contributions to the vacuum ultraviolet dual-comb spectroscopy measurements are characterized, guiding future efforts and technological development in this region.

Keywords: optical frequency comb, ultraviolet, molecular spectroscopy

The ultraviolet region of the electromagnetic spectrum contains a large number of strong atomic and molecular transitions originating directly from ground states that provide critical quantitative information needed for understanding fundamental processes and facilitating advances in science and technology. Although much progress has been made extending precision laser sources to the ultraviolet, the vacuum ultraviolet (VUV) ($10 < \lambda < 200$ nm)—where atmospheric gases such as O_2 strongly absorb [1]—has proved technically challenging for source generation and spectrometer design. Advances in high-resolution VUV spectroscopy impact a variety of industries and research fields. For example, spectroscopy of strong ultraviolet transitions in neutral and low ionization stages of atomic and molecular populations can greatly aid plasma diagnostics in many areas including monitoring of critical species in fusion reactors and degradation of plasma-facing materials [2], characterization of shock layer boundaries in hypersonics [3, 4], and studying effects of surface-plasma interactions on number densities of reactive species for medicine, surface decontamination [5], and semiconductor etching processes [6],

to name a few. Testing of fundamental physical laws, constants, and benchmarking quantum electrodynamics often rely on precision measurements of VUV transitions in simple molecules (e.g. H_2 , D_2) and direct measurements of Rydberg states [7, 8], multiply-charged ions [9], and even nuclear transitions [10]. Additionally, exoplanet research requires accurate and high-resolution VUV absorption cross-section data of molecular gases such as carbon dioxide, acetylene, and ammonia to inform models of the photochemistry induced by stellar radiation in the upper-atmospheres of these planets [11–14].

While several methods for VUV spectroscopy exist, each has its own limitations and complexities in addressing these applications. Dispersive spectrometers are suitable for many broadband studies [15], but require complex calibration for accurate measurements [16], and are ultimately limited in their spectral resolution [17]. VUV Fourier-transform spectrometers (FTS) have emerged offering higher resolution and simplified calibration for emission spectroscopy [18, 19] and isolated examples of absorption spectroscopy with a discharge light source [20]. However, for VUV FTS absorption spectroscopy, a synchrotron

beamline is often required for a coherent continuum source [21–23].

Twenty years ago, the first demonstrations of intracavity high harmonic generation (iHHG) extended optical frequency combs to the vacuum ultraviolet [24, 25]. Since then, many experiments have used iHHG to perform direct frequency comb spectroscopy in the VUV with unrivaled spectral resolution and absolute frequency calibration (see, for example [26–30]). Recently, high-precision measurements of the thorium nuclear isomer have showcased the impact of the VUV frequency comb [10]. With the possibility of a nuclear clock based on this transition [31, 32] comes the exciting prospect of testing our physical models through measurements of fundamental physical constants, and highlights the importance of precision VUV laser spectroscopy and source development [33–35].

However, a continuing limitation of VUV direct frequency comb spectroscopy is the difficulty, with only a single comb, of measuring multiple absorption features across the comb's broad bandwidth. This has limited direct comb spectroscopy in the VUV to narrow-band measurements of only sparse and well isolated transitions. To overcome this challenge at longer wavelengths, dual-comb spectroscopy (DCS) has proved to be a powerful method for broadband measurements of congested atomic and molecular spectra with resolution ultimately limited only by the linewidth of the individual comb teeth [36, 37]. In DCS, pulses from a pair of frequency combs with slightly different repetition frequencies ($\Delta f_{rep} = f_{rep,1} - f_{rep,2}$) are overlapped, building up an interferogram (IGM) as successive pulses step through each other. The Fourier transform of this IGM yields an optical spectrum down-converted to radio frequencies. DCS has many of the same

strengths as FTS, such as high resolution and broad bandwidth, with the additional simplicity of no moving parts and the capability for more rapid measurements of time-resolved events [38, 39]. Further, DCS provides absolute frequency measurements with high accuracy due to the coherent structure of the two optical frequency combs. However, DCS has previously been limited to longer wavelengths, only recently reaching the deep ultraviolet (DUV) ($200 < \lambda < 280$ nm) [40–46]. Here, we use iHHG of two ytterbium-based infrared combs to generate the DUV 5th harmonic ($\lambda = 210$ nm) and VUV 7th harmonic ($\lambda = 150$ nm) for DCS. At both harmonics, we demonstrate the capabilities of the DCS system with absolute frequency measurements of Doppler-resolved absorbance spectra of room-temperature molecular gases relevant to exoplanet photochemistry studies. This work extends the coverage of DCS to a previously inaccessible spectral regime, enabling fast and absolute frequency measurement capabilities with high spectral-resolution and bandwidth in the VUV.

1 Results

1.1 Intracavity High Harmonic Dual-Comb Spectrometer

The experimental schematic is shown in Fig. 1. A pair of home-built ytterbium fiber lasers generate near identical optical pulse trains with center wavelengths near $\lambda = 1050$ nm, repetition frequencies $f_{rep} = 77.8$ MHz, pulse durations of 150 fs, and average powers of 20 W. (see Methods for more details). These pulse trains are independently coupled into passive femtosecond enhancement cavities (fsECs) with similar cavity lengths, where intracavity average powers reach 5 kW [47, 48]. The

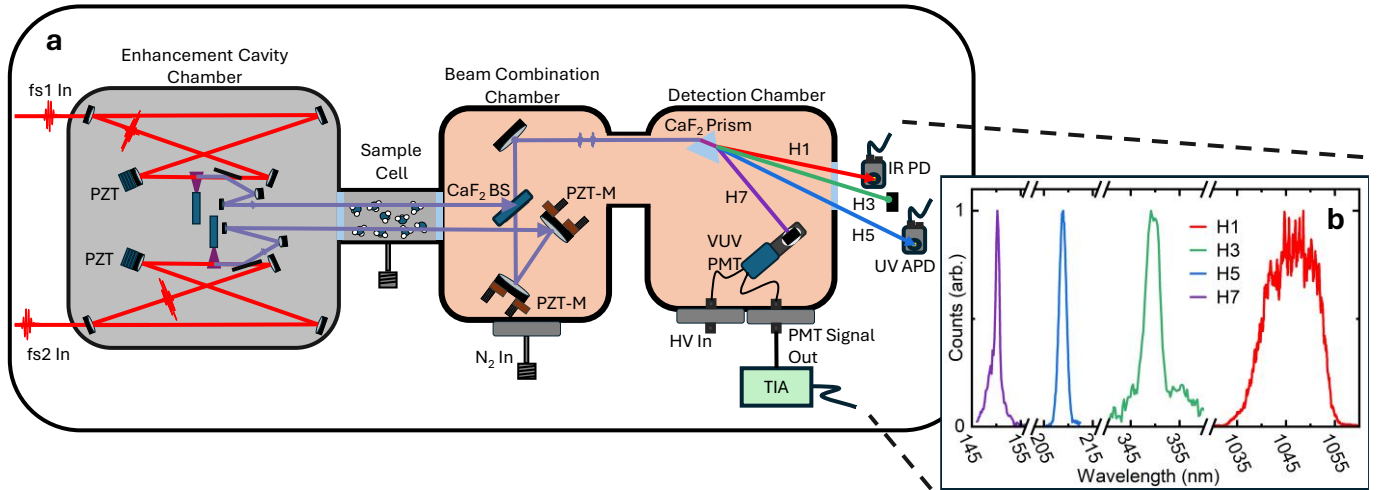


Fig. 1 Intracavity High Harmonic Generation and Dual-Comb Spectroscopy Beamline. **a**, Experimental schematic of intracavity high-harmonic generation showing each comb's out-coupled collinear harmonics aligned through a sample cell and into a nitrogen-purged chamber where they are overlapped on an ultraviolet beam splitter (BS) with piezo-controlled mirrors (PZT-M). Finally, the harmonics are separated with a CaF₂ prism, and the fundamental (H1) is measured on an infrared photodiode (IR PD), the 5th harmonic (H5) on an ultraviolet-enhanced avalanche photodiode (UV APD), and the 7th (H7) on a solar-blind photomultiplier tube (PMT). Vacuum chamber feed-throughs carry the high voltage (HV) bias to the PMT and output photocurrent from the PMT to an external trans-impedance amplifier (TIA). **b**, Low-resolution measurements of fundamental and harmonic spectra detected on various spectrometers.

Pound-Drever-Hall (PDH) technique is used to lock the length of each fsEC to the incident pulse train using fast piezo-electric transducers (PZTs) on fsEC mirrors. Xenon gas jets are introduced after the cavity foci, where peak intensities exceed $5 \times 10^{13} \text{ W/cm}^2$. High harmonic generation in the Xe gas generates odd harmonics of the fundamental, which are out-coupled with sapphire grazing incident plates (GIPs) at 70° angle of incidence. These GIPs have a high Fresnel reflectance across a broad bandwidth of s-polarized ultraviolet light with an anti-reflection coating for the fundamental beam ensuring low loss for the pulses circulating in the fsECs [49]. After the GIPs, the out-coupled harmonics are collimated by a curved mirror.

To achieve spatial overlap of the generated collinear harmonic pulse trains, we steer the beams through a CaF_2 -windowed sample cell and into a nitrogen purged chamber, using $\text{Al}+\text{MgF}_2$ coated mirrors, and combine them on a coated CaF_2 VUV beamsplitter. Piezo-actuated mirror mounts allow for fine tuning of the VUV spatial overlap while preserving the nitrogen purged environment. The harmonic orders of the combined beams are then spatially separated by a CaF_2 prism. The 7th harmonic VUV combs are detected using a solar-blind photomultiplier tube (PMT). The fundamental, 3rd, and 5th harmonics are picked off and aligned out of the combination chamber. The fundamental dual-comb IGMs are used for timing and triggering during data acquisition and the 5th is detected on a UV-extended silicon avalanche photodiode (APD). From the measured PMT photocurrent, we estimate the 7th harmonic power per comb on the detector to be $\sim 0.6 \mu\text{W}$, sufficient for dual-comb IGM detection. Taking into account the expected reflection and transmission losses from the optical elements in the VUV beamline, we conservatively estimate our out-coupled 7th harmonic VUV power to be $\sim 11.5 \mu\text{W}$ per comb. The low-resolution harmonic spectra, as shown in Fig. 1b, are measured on various spectrometers. The current dual-comb source extends to the VUV 7th harmonic; however, we expect the iHHG process is also producing significant powers of extreme ultraviolet harmonics ($\lambda < 120 \text{ nm}$) which are currently absorbed by use of CaF_2 transmissive optics.

1.2 Dual-Comb Characterization

With an evacuated sample cell, IGMs from the 5th harmonic APD and 7th harmonic PMT are recorded on a 14-bit digitizer with $\Delta f_{rep} = 147 \text{ Hz}$. We average the IGMs in time by measuring and correcting the envelope position and slow phase variation of the center-burst. In past UV studies, coherent averaging has been effective even with photon-limited power levels [46]. Here, the resonant conditions of the fsECs constrain the arbitrary selection of the combs' carrier-envelope-offset frequencies (f_{ceo}), a degree-of-freedom typically required for coherent averaging. Therefore, we must phase-correct IGMs individually before averaging, requiring the single-shot time-domain signal-to-noise ratio (SNR) of IGMs to be

> 1 . Fig. 2 shows representative single-shot IGMs and averages of 10,000 records.

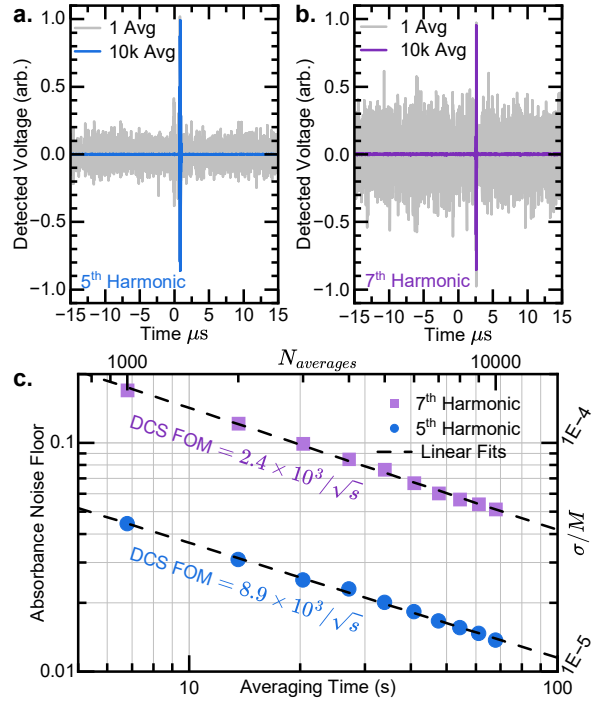


Fig. 2 Dual-Comb Interferogram Detection and Averaging
a-b, Detected 5th and 7th harmonic single-shot interferograms (gray) with centerbursts arbitrarily scaled to ± 1 unit are phase-corrected and averaged 10,000 times. **c**, For averaging time τ , the noise floor of the absorbance spectra decreases with $\sqrt{\tau}$. Here, both 5th and 7th harmonic interferograms are processed to resolve $M = 1000$ spectral elements across their respective optical bandwidths, giving $\Delta\nu_{res} = 4$ and 7 GHz, respectively.

For each harmonic, the averaged IGM is apodized by a Blackman-Harris window selected to achieve an intended instrument resolution. Here, the 5th (7th) harmonic has a resolution of 4 GHz (7 GHz) across its 4 THz (7 THz) bandwidth, resulting in $M = 1000$ frequency resolved elements in each harmonic spectrum. While the best resolution attainable from the full length, averaged IGM is ultimately limited only by the comb tooth spacing, f_{rep} , in these measurements we target resolving power that will be physically relevant to resolve Doppler-broadened molecular absorption features in measurements reported in Sections 1.3 and 1.4. The magnitude of the apodized IGM's Fourier transform gives a transmitted dual-comb power spectrum, which is normalized to a featureless absorbance spectrum and used to analyze the performance of the DUV and VUV DCS absorbance measurement. For 10,000 averages recorded in $\tau \sim 1$ minute, the standard deviation of the absorbance noise floor across the transmission spectrum's full-width at half-maximum reaches $\sigma = 0.015$ for the 5th harmonic and $\sigma = 0.05$ for the 7th. As shown in Fig. 2, the noise floor approaches these values with the expected $\sqrt{\tau}$ dependence [50]. From this performance, we calculate a DCS figure of merit as $\text{FOM} =$

$\frac{M}{\sigma\sqrt{\tau}} = 8.9 \times 10^3/\sqrt{s}$ for the 5th harmonic and $\text{FOM} = 2.4 \times 10^3/\sqrt{s}$ for the 7th. These results demonstrate that our DUV and VUV dual-comb spectrometer is capable of measuring molecular absorption with low minimum detectable absorbance and high signal to noise, with resolution sufficient for resolving typical molecular Doppler widths at room temperature.

1.3 5th Harmonic Acetylene Absorbance

Using the 5th harmonic of the DCS laser system, we target an absorption feature near $\lambda = 210$ nm in the $\tilde{A} \leftarrow \tilde{X}$ band of acetylene (C_2H_2) [13, 51] by tuning the center of each comb's infrared spectra to near $\lambda = 1050$ nm. We introduce a pressure $P = 50$ Torr of acetylene gas into a sample cell with length $L \sim 14$ cm. For this measurement, $\Delta f_{rep} = 101$ Hz. 10,000 IGMs are recorded, phase-corrected, averaged, and apodized to produce a single IGM. The retrieved dual-comb transmission spectrum (S_{sig}) is shown in Fig. 3a with a resolution of 4 GHz (0.6 pm) as determined by the apodization window.

The retrieved transmission spectrum is composed of radio-frequency (RF) carriers below $f_{rep}/2 = 39$ MHz. However, because the mutually-coherent combs are referenced to a continuous-wave (CW) laser of known optical frequency (see Methods), this RF transmission spectrum is self-calibrated to absolute optical frequency. The transmission spectrum shows many congested absorption features, and a pseudo-reference (S_{ref}) is constructed to match the background spectral shape. Finally, we calculate the absorbance spectrum $A = \ln(S_{ref}/S_{sig})$ shown in Fig. 3b. To validate our absolute frequency measurement of this acetylene absorption band, we compare to the acetylene cross-section measured with a resolution of 15 GHz on the Fourier-transform spectrometer DESIRS beamline at the SOLEIL synchrotron [13]. We observe excellent agreement in the independent wavelength calibration of the absorption spectra as shown in Fig. 3. Additionally, the previously reported cross-section of $4 \times 10^{-20} \text{ cm}^2$ for the

molecular band head near $\lambda = 209.7$ nm would predict an absorbance of $A = 1$, given the acetylene cell temperature and pressure, which is very near the measured absorbance.

1.4 7th Harmonic Ammonia Absorbance

Next, we use the VUV 7th harmonic to target an ammonia (NH_3) absorption feature in the $\tilde{B} \leftarrow \tilde{X}$ band centered at $\lambda = 149$ nm. From the previous 5th harmonic acetylene measurement, we tune our infrared comb spectra by $\Delta\lambda = 7$ nm, which tunes the VUV spectra of the 7th harmonic by 1 nm (13.5 THz) to overlap with this absorption feature. This adjustment is greater than the VUV bandwidth in any single position and demonstrates the wavelength agility of this approach for a targeted absorption study. A previously evacuated sample cell with length $L \sim 4.5$ cm is filled with a pressure $P = 0.8$ Torr of ammonia. For this measurement, $\Delta f_{rep} = 188$ Hz. With processing methods similar to the 5th harmonic absorbance study, 15,000 recorded 7th harmonic VUV IGMs are phase-corrected, averaged, and apodized to yield an absolute frequency transmission spectrum with a resolution of 7 GHz (0.5 pm) as shown in Fig. 4a. The absorbance spectrum, as shown in Fig. 4b, is again obtained from the transmission spectrum and a constructed pseudo-reference. A comparison of this first DCS VUV absorbance spectrum to the previously reported cross-section [14] demonstrates the quality of DCS in the VUV and its ability to resolve complex molecular absorption bands with absolute frequency calibration.

2 Discussion

While the DUV and VUV dual-comb spectrometer is already capable of resolving the absorption structure of room-temperature molecular gases, future developments will allow for improvements in the combination of SNR, resolution, and averaging times, which is characterized in the DCS FOM. To better understand the noise currently

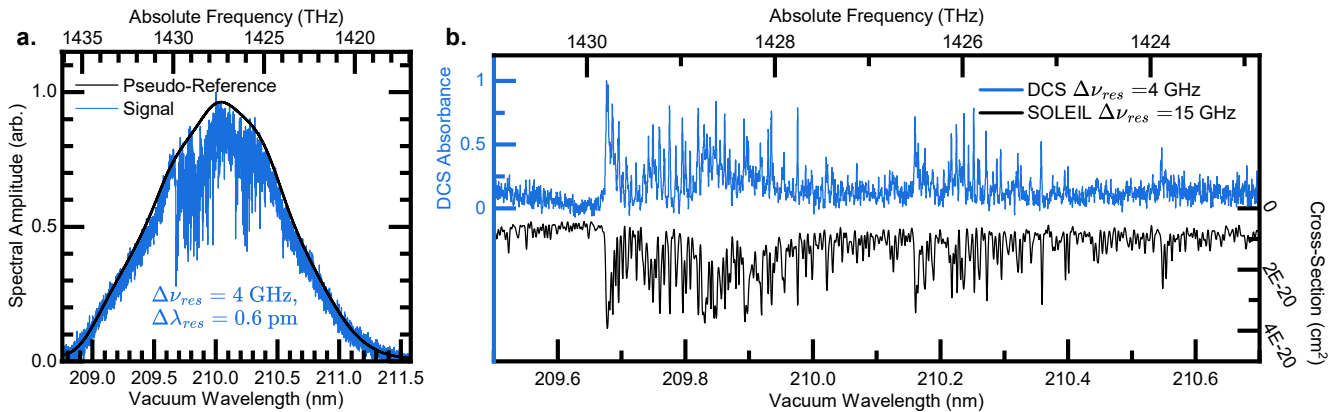


Fig. 3 Deep ultraviolet dual-comb spectroscopy of acetylene with the 5th harmonic at $\lambda = 210$ nm. a, The dual-comb transmission spectrum processed with a resolution of 4 GHz and 10,000 averages (blue) and a smoothed pseudo-reference (black). **b,** The dual-comb absorbance spectrum (blue) is compared to the absorption cross-section of acetylene (black) measured at the SOLEIL synchrotron with a resolution of 15 GHz [13].

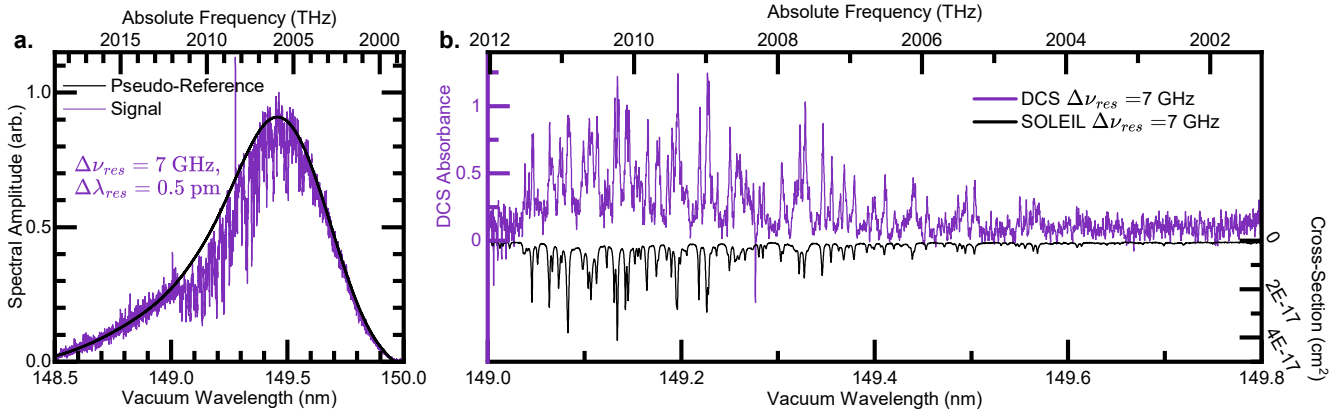


Fig. 4 Vacuum ultraviolet dual-comb spectroscopy of ammonia with the 7th harmonic at $\lambda = 149$ nm. **a**, The dual-comb transmission spectrum processed with a resolution of 7 GHz and 15,000 averages (purple) and a smoothed pseudo-reference (black). **b**, The dual-comb absorbance spectrum (purple) is compared to the absorption cross-section of ammonia (black) measured at the SOLEIL synchrotron with a resolution of 7 GHz [14].

dominating our measurement at the 7th harmonic, we calculate expected contributions from detection noise, shot noise, laser relative intensity noise (RIN), and dynamic range [50]. See Methods for details of these noise contribution calculations. Fig. 5 shows the expected SNR at various detected VUV comb powers (red) along with the SNR and VUV power of this initial demonstration (star). This measurement is dominated by detection noise and detection dynamic range.

The detection requirements of DCS are uniquely challenging for the VUV. In particular, a high sensitivity, low noise, high bandwidth detector is necessary. Here, we use a solar-blind PMT whose specifications do meet these requirements; however, the low PMT photocurrent is particularly susceptible to stray current noise pickup before it is converted to a more robust voltage signal by a sufficiently fast trans-impedance amplifier (TIA). We suspect that the stray current noise picked up in the vacuum chamber feed-through between the VUV PMT and external TIA is the main contributor to the detection noise limit and calculate its contribution, shown in Fig. 5. Additionally, the ratio of the PMT's maximum output current to this stray noise sets the detection dynamic range limit. In future experiments, more robust feed-through design and/or a fast, low noise, vacuum compatible TIA will improve these limits from the detection noise and the detection dynamic range. The latter of these will be further benefited by a higher maximum output current PMT. With these improvements, we estimate that the dual-comb FOM could increase by nearly an order of magnitude, yielding improvements in the SNR, resolution, and/or averaging time compared to measurements presented here. Alternatively, the quality of VUV DCS measurements would significantly improve with developments in the VUV detectors available with high bandwidth, high responsivity, and vacuum compatibility, such as VUV APDs.

With these detection improvements, increasing the detected VUV power will increase the dual-comb FOM

until reaching a limit from laser RIN. This RIN limit is conservatively estimated in Fig. 5 where shot noise contributions likely obscure the true RIN contribution. In the case of a RIN-limited measurement, VUV balanced detection would benefit performance further. We expect future measurements with increased VUV power on detector due to more efficient harmonic separation and other VUV beamline improvements. While out-coupled 7th harmonic VUV power exceeding 10 μ W is sufficient for the measurements presented here, in other measurements we out-coupled over 20 μ W per 7th harmonic VUV comb by increasing xenon backing pressure. However, this higher VUV power introduces additional difficulties for long acquisition periods and is not particularly impactful before first addressing the above detection limitations.

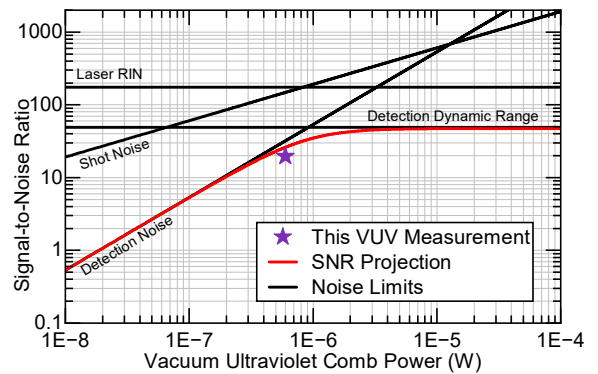


Fig. 5 Vacuum ultraviolet dual-comb spectroscopy noise analysis. For $M = 1000$ frequency-resolved elements ($\Delta\nu_{res} = 7$ GHz resolution across $\Delta\nu_{BW} = 7$ THz optical bandwidth), $\tau = 68$ s averaging time, and 0.6 μ W power on detector per comb, our vacuum ultraviolet dual-comb measurement has an SNR near 20 (star). Projected SNR at other detected comb powers (red) is calculated from various noise source contributions (black).

These results demonstrate DCS in the VUV for the first time. We resolve the Doppler-broadened line widths of complex molecular absorbance spectra with high SNR.

The absolute frequency and photometric accuracy of the DCS system will allow for further targeted absorption cross-section studies in the VUV with modest table-top infrastructure. Additionally, iHHG dual-comb sources provide a scalable approach for extending DCS even farther into the extreme ultraviolet. This regime, beyond the transmission band of CaF₂ optics, can make use of previously demonstrated wavefront-division beamsplitters and Fresnel zone plate optics [17, 30] to overlap and record IGMs of higher harmonics. The establishment of DCS in the VUV provides a powerful spectroscopic method in this challenging spectral regime, enabling fast acquisition, absolute frequency accuracy, broad bandwidth, and spectral resolution limited only by the linewidth of the comb teeth. The ability to precisely probe complex atomic and molecular quantum structure and dynamics through excitation of high energy transitions directly from the ground state opens new opportunities for quantitative measurements that can have a dramatic impact in fields ranging from plasma diagnostics to astrophysics and fundamental science.

References

- [1] Standardization, I.O.: ISO 21348 definitions of solar irradiance spectral categories. *Environment* **5**, 6–7 (2007)
- [2] Béchu, S., Lemaire, J., Gavilan, L., Aleiferis, S., Shakhatov, V., Lebedev, Y.A., Fombaron, D., Bonny, L., Menu, J., Bès, A., *et al.*: Direct measurements of electronic ground state ro-vibrationally excited D₂ molecules produced on ECR plasma-facing materials by means of VUV-FT absorption spectroscopy. *Journal of Quantitative Spectroscopy and Radiative Transfer* **257**, 107325 (2020)
- [3] Holloway, M.E., Boyd, I.D.: Sensitivity analysis of thermochemical kinetics modeling for hypersonic air flows. *Journal of Thermophysics and Heat Transfer* **36**(3), 584–593 (2022)
- [4] Krish, A., Streicher, J.W., Hanson, R.K.: Spectrally-resolved ultraviolet absorption measurements of shock-heated NO from 2000 K to 6000 K for the development of a two-color rotational temperature diagnostic. *Journal of Quantitative Spectroscopy and Radiative Transfer* **280**, 108073 (2022)
- [5] Peverall, R., Ritchie, G.A.: Spectroscopy techniques and the measurement of molecular radical densities in atmospheric pressure plasmas. *Plasma Sources Science and Technology* **28**(7), 073002 (2019)
- [6] Hori, M., Goto, T.: Progress of radical measurements in plasmas for semiconductor processing. *Plasma Sources Science and Technology* **15**(2), 74 (2006)
- [7] Hussels, J., Hölsch, N., Cheng, C.-F., Salumbides, E.J., Bethlem, H.L., Eikema, K.S., Jungen, C., Beyer, M., Merkt, F., Ubachs, W.: Improved ionization and dissociation energies of the deuterium molecule. *Physical Review A* **105**(2), 022820 (2022)
- [8] Roth, C., Velasco, A.M., Gründeman, E.L., Collombon, M., Beyer, M., Barbe, V., Eikema, K.S.: High-precision Ramsey-comb spectroscopy on molecular deuterium for tests of molecular quantum theory. *Molecular Physics* **121**(17–18), 2211405 (2023)
- [9] Berengut, J., Dzuba, V., Flambaum, V., Ong, A.: Electron-hole transitions in multiply charged ions for precision laser spectroscopy and searching for variations in α . *Physical review letters* **106**(21), 210802 (2011)
- [10] Zhang, C., Ooi, T., Higgins, J.S., Doyle, J.F., Wense, L., Beeks, K., Leitner, A., Kazakov, G.A., Li, P., Thirolf, P.G., *et al.*: Frequency ratio of the ^{229m}Th nuclear isomeric transition and the ⁸⁷Sr atomic clock. *Nature* **633**(8028), 63–70 (2024)
- [11] Venot, O., Fray, N., Bénilan, Y., Gazeau, M.-C., Hébrard, E., Larcher, G., Schwell, M., Dobrijevic, M., Selsis, F.: High-temperature measurements of VUV-absorption cross sections of CO₂ and their application to exoplanets. *Astronomy & Astrophysics* **551**, 131 (2013)
- [12] Ranjan, S., Schwieterman, E.W., Harman, C., Fateev, A., Sousa-Silva, C., Seager, S., Hu, R.: Photochemistry of anoxic abiotic habitable planet atmospheres: impact of new H₂O cross sections. *The Astrophysical Journal* **896**(2), 148 (2020)
- [13] Fleury, B., Poveda, M., Benilan, Y., Veillet, R., Venot, O., Tremblin, P., Fray, N., Gazeau, M.-C., Schwell, M., Jolly, A., *et al.*: High-temperature measurements of acetylene VUV absorption cross sections and application to warm exoplanet atmospheres. *Astronomy & Astrophysics* **693**, 82 (2025)
- [14] Pratt, S.T., Jacovella, U., Boyé-Péronne, S., Ashfold, M.N., Joyeux, D., De Oliveira, N., Holland, D.M.: High-resolution absorption spectroscopy of room-temperature and jet-cooled ammonia between 59,000 and 93,000 cm⁻¹. *Journal of Molecular Spectroscopy* **396**, 111810 (2023)
- [15] Trichard, F., Moncayo, S., Devismes, D., Pelascini, F., Maurelli, J., Feugier, A., Sasseville, C., Surma, F., Motto-Ros, V.: Evaluation of a compact VUV spectrometer for elemental imaging by laser-induced breakdown spectroscopy: Application to mine core characterization. *Journal of Analytical Atomic Spectrometry* **32**(8), 1527–1534 (2017)

[16] Fröhler-Bachus, C., Friedl, R., Briefi, S., Fantz, U.: Absolute radiometric calibration of a VUV spectrometer in the wavelength range 46–300 nm. *Journal of Quantitative Spectroscopy and Radiative Transfer* **259**, 107427 (2021)

[17] Samson, J.A., Ederer, D.L.: Vacuum ultraviolet spectroscopy. Academic press (2000)

[18] Thorne, A., Harris, C., Wynne-Jones, I., Learner, R., Cox, G.: A Fourier transform spectrometer for the vacuum ultraviolet: design and performance. *Journal of Physics E: scientific instruments* **20**(1), 54 (1987)

[19] Griesmann, U., Kling, R., Burnett, J.H., Bratasz, L.: NIST FT700 vacuum ultraviolet Fourier transform spectrometer: applications in ultraviolet spectrometry and radiometry. In: *Ultraviolet Atmospheric and Space Remote Sensing: Methods and Instrumentation II*, vol. 3818, pp. 180–188 (1999). SPIE

[20] Murray, J., Yoshino, K., Esmond, J., Parkinson, W., Sun, Y., Dalgarno, A., Thorne, A.P., Cox, G.: Vacuum ultraviolet fourier transform spectroscopy of the δ (0, 0) and β (7, 0) bands of NO. *The Journal of chemical physics* **101**(1), 62–73 (1994)

[21] Yoshino, K., Smith, P., Parkinson, W., Thorne, A., Ito, K.: The combination of a VUV Fourier-transform spectrometer and synchrotron radiation. *Review of scientific instruments* **66**(2), 2122–2124 (1995)

[22] Matsui, T., Cheung, A.-C., Leung, K.-S., Yoshino, K., Parkinson, W., Thorne, A., Murray, J., Ito, K., Imajo, T.: High resolution absorption cross-section measurements of the schumann–runge bands of O₂ by VUV Fourier transform spectroscopy. *Journal of Molecular Spectroscopy* **219**(1), 45–57 (2003)

[23] De Oliveira, N., Roudjane, M., Joyeux, D., Phalippou, D., Rodier, J.-C., Nahon, L.: High-resolution broad-bandwidth Fourier-transform absorption spectroscopy in the VUV range down to 40 nm. *Nature Photonics* **5**(3), 149–153 (2011)

[24] Jones, R.J., Moll, K.D., Thorpe, M.J., Ye, J.: Phase-coherent frequency combs in the vacuum ultraviolet via high-harmonic generation inside a femtosecond enhancement cavity. *Physical Review Letters* **94**(19), 193201 (2005)

[25] Gohle, C., Udem, T., Herrmann, M., Rauschenberger, J., Holzwarth, R., Schuessler, H.A., Krausz, F., Hänsch, T.W.: A frequency comb in the extreme ultraviolet. *Nature* **436**(7048), 234–237 (2005)

[26] Ozawa, A., Rauschenberger, J., Gohle, C., Herrmann, M., Walker, D.R., Pervak, V., Fernandez, A., Graf, R., Apolonski, A., Holzwarth, R., *et al.*: High harmonic frequency combs for high resolution spectroscopy. *Physical review letters* **100**(25), 253901 (2008)

[27] Yost, D.C., Schibli, T.R., Ye, J., Tate, J.L., Hostetter, J., Gaarde, M.B., Schafer, K.J.: Vacuum-ultraviolet frequency combs from below-threshold harmonics. *Nature Physics* **5**(11), 815–820 (2009)

[28] Bernhardt, B., Ozawa, A., Vernaleken, A., Pupeza, I., Kaster, J., Kobayashi, Y., Holzwarth, R., Fill, E., Krausz, F., Hänsch, T.W., *et al.*: Vacuum ultraviolet frequency combs generated by a femtosecond enhancement cavity in the visible. *Optics letters* **37**(4), 503–505 (2012)

[29] Ozawa, A., Kobayashi, Y.: VUV frequency-comb spectroscopy of atomic xenon. *Physical Review A—Atomic, Molecular, and Optical Physics* **87**(2), 022507 (2013)

[30] Benko, C., Allison, T.K., Cingöz, A., Hua, L., Labaye, F., Yost, D.C., Ye, J.: Extreme ultraviolet radiation with coherence time greater than 1 s. *Nature Photonics* **8**(7), 530–536 (2014)

[31] Elwell, R., Schneider, C., Jeet, J., Terhune, J.E.S., Morgan, H.W.T., Alexandrova, A.N., Tran Tan, H.B., Derevianko, A., Hudson, E.R.: Laser excitation of the ²²⁹Th nuclear isomeric transition in a solid-state host. *Phys. Rev. Lett.* **133**, 013201 (2024)

[32] Tiedau, J., Okhapkin, M.V., Zhang, K., Thielking, J., Zitzer, G., Peik, E., Schaden, F., Pronebner, T., Morawetz, I., De Col, L.T., Schneider, F., Leitner, A., Pressler, M., Kazakov, G.A., Beeks, K., Sikorsky, T., Schumm, T.: Laser excitation of the Th-229 nucleus. *Phys. Rev. Lett.* **132**, 182501 (2024)

[33] Uzan, J.-P.: Varying constants, gravitation and cosmology. *Living reviews in relativity* **14**(1), 1–155 (2011)

[34] Flambaum, V.V.: Enhancing the effect of Lorentz invariance and Einstein’s equivalence principle violation in nuclei and atoms. *Phys. Rev. Lett.* **117**, 072501 (2016)

[35] Safronova, M., Budker, D., DeMille, D., Kimball, D.F.J., Derevianko, A., Clark, C.W.: Search for new physics with atoms and molecules. *Reviews of Modern Physics* **90**(2), 025008 (2018)

[36] Coddington, I., Newbury, N., Swann, W.: Dual-comb spectroscopy. *Optica* **3**(4), 414–426 (2016)

[37] Picqué, N., Hänsch, T.W.: Frequency comb spectroscopy. *Nature Photonics* **13**(3), 146–157 (2019)

[38] Bergevin, J., Wu, T.-H., Yeak, J., Brumfield, B.E., Harilal, S.S., Phillips, M.C., Jones, R.J.: Dual-comb spectroscopy of laser-induced plasmas. *Nature communications* **9**(1), 1273 (2018)

[39] Zhang, Y., Weeks, R.R., Lecaplain, C., Harilal, S.S., Yeak, J., Phillips, M.C., Jones, R.J.: Burst-mode dual-comb spectroscopy. *Optics Letters* **46**(4), 860–863 (2021)

[40] McCauley, J.J., Phillips, M.C., Weeks, R.R., Zhang, Y., Harilal, S.S., Jones, R.J.: Dual-comb spectroscopy in the deep ultraviolet. *Optica* **11**(4), 460–463 (2024)

[41] Hofer, T., Hehl, G., Meyer, J.G., Pronin, O.: Free-running deep-UV dual-comb spectroscopy. *Journal of Physics B: Atomic, Molecular and Optical Physics* **58**(10), 105403 (2025)

[42] Li, Q., Bai, H., Teng, X., Chen, H., Mai, H., Zhang, Z., Zhang, J., Xuan, H.: Deep ultraviolet dual comb from a thin-disk laser. *Ultrafast Science* **5**, 0087 (2025)

[43] Chang, K.F., Lesko, D.M., Mashburn, C., Chang, P., Tsao, E., Lind, A.J., Diddams, S.A.: Multi-harmonic near-infrared–ultraviolet dual-comb spectrometer. *Optics Letters* **49**(7), 1684–1687 (2024)

[44] Fürst, L., Kirchner, A., Eber, A., Siegrist, F., Vora, R., Bernhardt, B.: Broadband near-ultraviolet dual comb spectroscopy. *Optica* **11**(4), 471–477 (2024)

[45] Muraviev, A., Konnov, D., Vasilyev, S., Vodopyanov, K.L.: Dual-frequency-comb UV spectroscopy with one million resolved comb lines. *Optica* **11**(11), 1486–1489 (2024)

[46] Xu, B., Chen, Z., Hänsch, T.W., Picqué, N.: Near-ultraviolet photon-counting dual-comb spectroscopy. *Nature* **627**(8003), 289–294 (2024)

[47] Jones, R.J., Diels, J.-C., Jasapara, J., Rudolph, W.: Stabilization of the frequency, phase, and repetition rate of an ultra-short pulse train to a fabry–perot reference cavity. *Optics communications* **175**(4-6), 409–418 (2000)

[48] Jones, R.J., Ye, J.: Femtosecond pulse amplification by coherent addition in a passive optical cavity. *Optics letters* **27**(20), 1848–1850 (2002)

[49] Fischer, J., Drs, J., Labaye, F., Modsching, N., Müller, M., Wittwer, V.J., Südmeyer, T.: Efficient XUV-light out-coupling of intra-cavity high harmonics by a coated grazing-incidence plate. *Optics Express* **30**(17), 30969–30979 (2022)

[50] Newbury, N.R., Coddington, I., Swann, W.: Sensitivity of coherent dual-comb spectroscopy. *Optics express* **18**(8), 7929–7945 (2010)

[51] Bénilan, Y., Smith, N., Jolly, A., Raulin, F.: The long wavelength range temperature variations of the mid-UV acetylene absorption coefficient. *Planetary and Space Science* **48**(5), 463–471 (2000)

[52] Martinez, O.: 3000 times grating compressor with positive group velocity dispersion: Application to fiber compensation in 1.3–1.6 μm region. *IEEE Journal of Quantum Electronics* **23**(1), 59–64 (1987)

3 Methods

3.1 Infrared Comb Source

Each home-built frequency comb originates from a nonlinear-polarization-rotation mode-locked ytterbium-doped fiber oscillator whose output is amplified in a dual-clad fiber preamplifier. The average power output of the amplifier is nominally 1 – 2 W. The pulses are stretched to ~ 2 ps pulse duration and spectrally filtered using a Martinez-stretcher [52], providing control over the portion of the spectrum to be amplified by the subsequent photonic crystal fiber power amplifier (PCF). The commercial PCF module generates up to 50 W of average power, although we have only used outputs near to 20 W in the current experiments. The pulses are compressed to durations of ~ 150 fs and coupled into the fsEC. We estimate our enhancement factor to be 250 giving ~ 5 kW average intracavity power, with a beam diameter of approximately ~ 22 μm at the cavity focus. Shortly after the cavity focus we introduce a xenon gas jet where the peak intensity exceeds 5×10^{13} W/cm², which is sufficient to drive the high harmonic process. The gas jet originates from a glass capillary with inner diameter of 100 μm with a xenon backing pressure near 1500 Torr. The gas jets are on piezo-driven translation stages to achieve optimal harmonic yield.

We establish the mutual coherence necessary for DCS measurements between these two combs with optical phase locks of comb teeth to two CW reference lasers at $\lambda = 1050$ and 1064 nm. These CW references are themselves pre-stabilized to a common reference cavity with PDH locking. Additionally, the absolute frequency of one of the CW references is measured precisely on an infrared wavemeter with accuracy of 0.3 GHz.

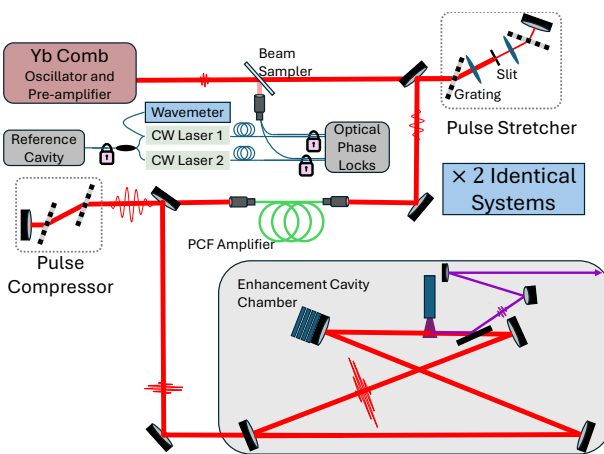


Fig. 6 Ytterbium Comb Schematic. Illustration of the beam-path from an ytterbium fiber oscillator and pre-amplifier, through the pulse stretcher, photonic crystal fiber (PCF) amplifier, and pulse compressor before reaching the passive enhancement cavity. Comb modes are controlled with optical phase locks to pre-stabilized continuous-wave (CW) reference lasers, one of which is measured on a wavemeter.

3.2 Absolute Frequency Calibration

Because the interference of two optical frequency combs can have a one-to-one mapping from the optical to the RF, we can independently calibrate the absolute optical frequency of our dual-comb measurements. In our current configuration we use two optical locks to stabilize our comb modes. By measuring the comb repetition frequencies, the absolute frequency of one of the CW references with a wavemeter, and the offset phase locks of the combs to this reference, we know the absolute frequencies of all comb modes. Since the high harmonic process generates sum-frequency harmonics from these comb modes, we therefore have precise knowledge of the VUV comb modes as well. By choosing a sufficiently small Δf_{rep} (~ 150 Hz) each heterodyne interference frequency from these known comb modes maps to a unique RF frequency less than $f_{rep}/2$. This one-to-one correspondence allows us to calibrate the RF-domain measurements directly to the VUV absolute optical frequencies prior to any comparisons with other VUV references or absorption line positions.

3.3 Dual-Comb Noise Calculations

As discussed in Section 2, we calculate expected noise contributions from several sources to understand the limitations in the VUV measurement presented here and to project potential SNR of future measurements with improved devices and more VUV power on detector. Here, we describe the details of these calculations derived from standard DCS theoretical framework [50]. Considering the DCS noise to arise from four sources—detection noise, shot noise, RIN, and dynamic range—we expect a noise level

$$\sigma = \frac{M\sqrt{\epsilon}}{0.8\sqrt{\tau}} \sqrt{a_{NEP}/P_c^2 + a_{range} + a_{shot}/P_c + a_{RIN}}$$

for M frequency resolved elements, duty cycle $\epsilon = \Delta\nu_{res}/f_{rep}$, averaging time τ , single comb power on detector P_c , and noise contributions a_i .

For detection noise, we are limited by stray current noise $I_{rms} \sim 1.3$ μA through the vacuum chamber feed-through between the PMT and external TIA. This current noise limits the noise equivalent power term to $a_{NEP} = 1.7 \times 10^{-22}$ W²/Hz. The ratio of this stray current noise to the 100 μA maximum output current of the PMT sets the detection dynamic range to be $a_{range} = 2 \times 10^{-10}$ 1/Hz. The PMT used has a quantum efficiency at $\lambda = 150$ nm of 40%, so the shot noise contribution is $a_{shot} = 1.3 \times 10^{-17}$ W/Hz. Finally, the VUV laser RIN is measured to be -114 dBc/Hz and fairly constant across the relevant dual-comb carriers, giving the RIN contribution to be $a_{RIN} = 1.6 \times 10^{-11}$ 1/Hz.

With $P_c \sim 0.6$ μW per VUV comb on detector, these terms predict a dual-comb noise limit of $\sigma = 0.04$ for $M = 1000$ frequency resolved elements with $\tau = 68$ s of averaging time, very near the 0.05 VUV noise limit we measure shown in Fig. 2. Additionally, from these terms

and the above equation for σ , it is straightforward to predict the dual-comb noise limit for various VUV powers on detector or given improvements to detection noise or laser RIN mitigation, as shown in Fig. 5 and surrounding discussion.

Supplementary information Not applicable

Acknowledgements The authors thank Eric R. Hudson and James E. S. Terhune for assistance with the VUV PMT. The authors thank Kelby B. Todd for helpful discussions and gas handling assistance.

Declarations

Funding Funding support provided by Air Force Office of Scientific Research [FA9550-20-1-0273]. JJM was funded

through the National Defense Science and Engineering Graduate Fellowship Program.

Conflict of interest/Competing interests The authors have no conflict of interest to disclose.

Ethics approval and consent to participate Not applicable

Consent for publication Not Applicable

Data availability Available upon reasonable request.

Materials availability Not Applicable

Code availability Not Applicable